Effects of Cope Geometry on the Strength and Behavior of Cellular and Castellated Beams

R.M. HOFFMAN, D.W. DINEHART, S.P. GROSS, J.R. YOST, and J.M. HENNESSEY

Castellated and cellular beams, steel beams with hexagonal and circular web openings, respectively, have been used in European structures since the 1940s. Acceptance of these beams has been much slower in the United States due to an initial lack of comprehensive design standards. However, due to their design and construction advantages, engineers are increasingly utilizing open web sections in their designs. Design advantages include a reduced weight per unit length of beam and an improved flexural stiffness (larger section modulus) resulting from the increased depth, thus allowing longer spans, which provide for a more open floor plan. Construction advantages include the ability to run utilities through the castellations, which can save several inches of floor-to-floor height. The open webs also provide aesthetic advantages when used in structures with exposed beams. Open web sections are considered to be particularly economical in structures that have medium to high design loads over medium to long spans. Recent applications of castellated and cellular beams range from commercial and industrial buildings to parking garages. (Hennessey, Dinehart, Hoffman, Gross and Yost, 2004)

The recent increase in usage of castellated and cellular beams highlights the need for additional research. Present design standards for open web beams in the United States remain nonuniform, hampering the ability of engineers to efficiently use these sections despite their advantages. This incomplete treatment of castellated beams in design codes is, in part, a result of the limited research on these types of beams. Prior experimental work conducted on these beams involved a minimal number of test specimens, making it difficult to determine how indicative the test results are of true castellated beam behavior.

R.M. Hoffman is an assistant professor, department of mechanical engineering, Villanova University, Villanova, PA.

D.W. Dinehart is an associate professor, department of civil and environmental engineering, Villanova University, Villanova, PA.

S.P. Gross is an associate professor, department of civil and environmental engineering, Villanova University, Villanova, PA.

J.R. Yost is an associate professor, department of civil and environmental engineering, Villanova University, Villanova, PA.

J.M. Hennessey is a structural engineer, DMJM Harris, Philadelphia, PA.

BACKGROUND AND THEORY

Design codes throughout England and Europe, where the use of castellated beams is more common, have established some general standards for the design of castellated beams; however, there is no standard reference in the United States for the design and analysis of these sections. Consequently, the design and analysis of these beams is based on a combination of several sources, including the European codes (Ward, 1990), research findings, and structural theory.

Boyer (1964) was among the first to investigate the design practices and analysis of castellated beams. His work focused primarily on critical assumptions made in the design and analysis process, where he noted that because the longitudinal fiber stresses of castellated beams are influenced by both bending moment and vertical shear, they should be analyzed as Vierendeel trusses. Based on simply supported end conditions and a uniformly distributed load, Blodgett (1966) proposed design checks for bending and shear stresses as well as web-post buckling due to both horizontal shear and compressive forces. Many of the design and analysis concepts that are employed today are based on Blodgett's work. Aglan and Redwood (1974) studied web-post buckling further, incorporating plasticity and strain hardening. None of the theoretical or design equations derived in the aforementioned work account for the effect of cope geometries on the buckling behavior or ultimate strength of the beam.

Similarly, in the experimental research conducted on castellated and cellular beams in the past fifty years, none has provided insight into how cope geometries affects beam strength and failure. Gibson and Jenkins (1957) and Toprac and Cooke (1959) conducted experimental studies on uncoped simply supported castellated beams with point loads. Other researchers have conducted experimental investigations aimed at determining the adequacy of using a Vierendeel model to predict the behavior of castellated beams (Kolosowski, 1964; Douty and Baldwin, 1966; Mandel, Brennan, Wasil and Antoni, 1971). Other researchers have conducted experimental tests on castellated beams with the goal of investigating buckling failures: local, web-post, and lateral torsional (Hosain and Speirs, 1973; Surtees and Liu, 1995).

Zaarour and Redwood, 1996, studied web buckling of thin-webbed castellated beams by comparing experimental test results to a finite element analysis. The test results demonstrated that web-post buckling was a real possibility for practical beam dimensions and must be included in design procedures. The finite element results provided a good prediction of the strength of beams controlled by web instability. In a continuation of this work, Redwood and Demirdjian (1998) investigated web-post buckling due to shear. All of the specimens were simply supported and loaded by a single point load slightly offset from midspan. The critical loads given by the elastic finite element analysis showed a slight reduction as the number of openings included in the model increased. A parametric study was conducted to investigate web-buckling behavior near the end of a castellated beam. Elastic buckling coefficients giving the shearing force at buckling of the web-post for a variety of geometries were presented.

All of these studies utilized simple roller supports and uncoped castellated beams. Most of the studies used point loads, as opposed to a uniformly distributed load, the basis for analysis used by Blodgett (1966). These experimental conditions fail to adequately model conditions commonly found in practice, namely, uniform load and bolted connections. Further, few studies have dealt with finite element modeling of castellated beams; the modeling that has been reported has focused primarily on web-post behavior. None of these studies has investigated the behavior of cellular beams.

Recent experimental research conducted on coped cellular and castellated beams with bolted shear tab connections (Aloi, Gross, Dinehart and Yost, 2002; Reiter, Dinehart, Gross and Yost, 2002) shows that these beams often fail in one of three ways when subjected to a uniformly distributed load: (1) by buckling of the first web-post, (2) by buckling of the *e′* region, or (3) by a combination of *e′* region buckling and web-post buckling. The web-post and *e′* regions are illustrated in Figure 1. This paper details an experimental and analytical study conducted on coped steel beams with expanded hexagonal and circular web sections. The goal of this study is to determine the effect of the *e′* distance on the strength and behavior of cellular and castellated beams.

EXPERIMENTAL TESTING PROGRAM

The experimental program consisted of testing 36 ASTM A570 Grade 50 steel noncomposite open web expanded beams with varied cope geometries and depths. The test specimens were divided into two beam types, castellated or cellular, with three different depths per type and three different cope dimensions per depth. This test matrix resulted in 18 unique designs with two identical specimens per design. All specimens spanned 15.0625 ft. (180.75 in.). The designations and significant dimensions can be found in Table 1.

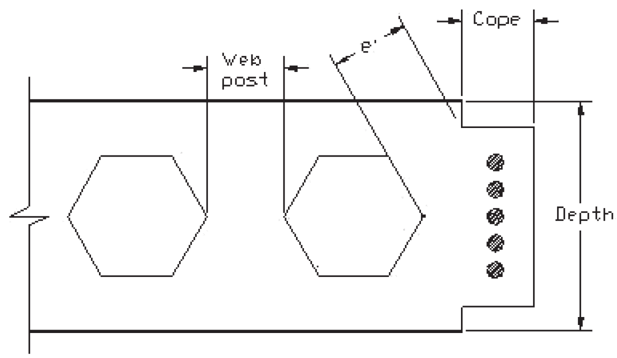

(a) Castellated beam

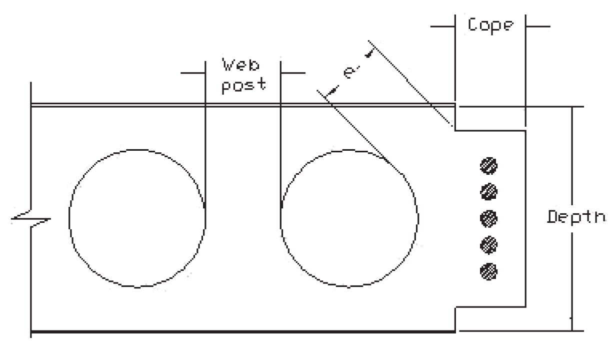

(b) Cellular beam

Fig. 1. Beam sections showing e' and first web-post regions.

Table 1: Beam Dimensions and Designations				
Specimen #	Root Beam	Top Cape (length × depth)	e' distance (in.)	Depth (in.)
Castellated Beams				
CB 1-1	W12×35	3 × 5	3.33	18.1
CB 1-2		3 × 6	2.47	
CB 1-3		3 × 5.5	3.03	
CB 2-1	W14×22	3 × 5.5	4.87	20.6
CB 2-2		3 × 6	4.44	
CB 2-3		3 × 6.5	4.04	
CB 3-1	W16×31	3 × 5.5	6.36	23.8
CB 3-2		3 × 5.75	6.15	
CB 3-3		3 × 6.5	5.51	
Cellular Beams				
LB 1-1	W12×35	3 × 5	2.63	18
LB 1-2		3 × 6	1.88	
LB 1-3		3 × 5.5	2.25	
LB 2-1	W14×22	3 × 5.5	3.69	20.8
LB 2-2		3 × 6	3.31	
LB 2-3		3 × 6.5	2.94	
LB 3-1	W16×31	3 × 5.5	5.06	23.6
LB 3-2		3 × 5.75	4.88	
LB 3-3		3 × 6.5	4.31	

The beams were tested in a self-reacting frame. The support conditions for each specimen consisted of a double-angle bolted connection utilizing two-L4×4×⅜ bolted to the flange of a W10×26 stub column. The beams were bolted to the double-angle connection using four ¾-in.-diameter bolts at each end. To prevent rotation of the specimen about the longitudinal axis, lateral bracing was provided at the ends and the third points of the span for both the top and bottom flanges. A castellated beam prepared for testing is shown in Figure 2.

All specimens were subjected to concentrated loads spaced at 6 in. The point loads were applied using 13 20-kip hydraulic cylinders spaced 12 in. apart. The cylinder load was further distributed over the beam by the use of spreader plates reducing the load spacing to every 6 in. along the specimen. The load was applied using a manual two-speed hydraulic pump at a rate of approximately 1 kip/min. Loading continued until an approximate 10% decrease from the maximum load was observed.

For each beam in the experimental program, load, vertical deflection and strain were recorded. Load was recorded for each test specimen by two 20-kip amplified load cells placed directly under the hydraulic cylinders at each end. Vertical deflection was measured at four points along the span of each beam with linear variable-differential transformers (LVDT). One LVDT was placed under each connection and at the quarter-span and midspan of each beam. Strains were measured throughout the e' region and at various points along the beam using strain rosettes and uniaxial strain gages. The e' region of the test specimens was instrumented with between three and five strain rosettes. Yielding of the steel beam was mapped visually using a lime wash on the noninstrumented side of the beam.

ANALYTICAL MODELING

Nonlinear finite element (FE) models were constructed in ANSYS 7.0 for each of the 18 beams listed in Table 1. As can be seen in Figure 3, the beam was modeled as symmetric about its midlength with out-of-plane constraints applied to the top and bottom flanges at the end and the third-point to model the lateral bracing in the experiments. A bilinear isotropic material model (elastic modulus, E = 29,000 ksi; tangent modulus, E_T = 60 ksi) with von Mises yield criterion (yield strength, F_y = 55 ksi) was used for the steel to model the nonlinear material behavior of the beam. The material properties used in the models were determined via tensile testing using coupons taken from the test beams. All tension tests were conducted in accordance with ASTM E8 (ASTM, 1989).

The primary objective of the FE analysis was to determine beam behavior in the e' region; consequently, significant attention was focused on properly modeling the connection of the beam to the loading frame. For the model, the two L4×4×⅜ angles were included. The beams were connected to the double angles via a simplified bolt model. This bolt model coupled the nodes at the bolt locations such that these nodes would displace in all directions as a single unit. Contact without friction was then defined between the beam and the angles. In the experimental testing, the back face of these

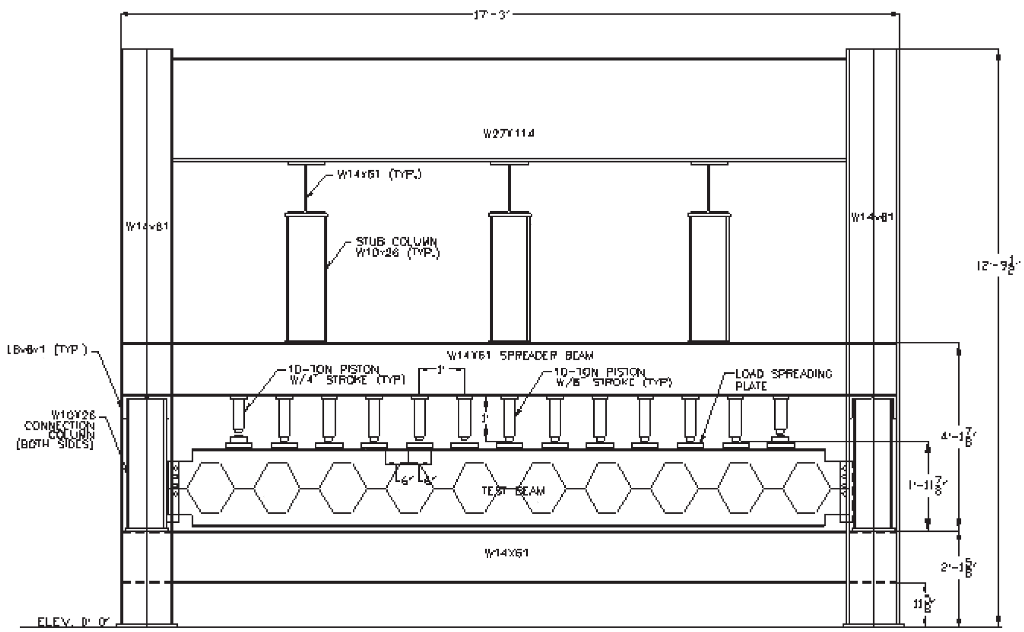

Fig. 2. Castellated beam in self-reacting frame.

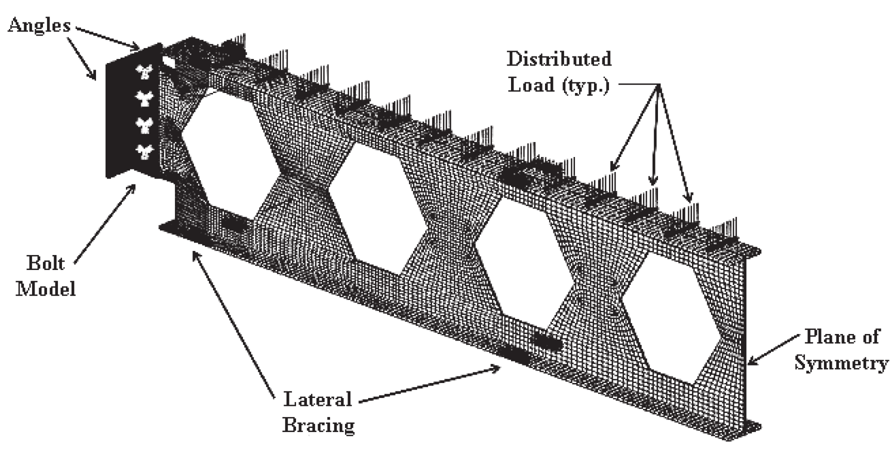

Fig. 3. Representative finite element model for buckling analysis.

angles were bolted, using seven ¾ in. bolts per angle, to the flange of the W10x26 stub column, which was fixed on both ends to the test frame. The short length of the stub column coupled with its large moment of inertia resulted in a flexurally stiff attachment point for the angles. As such, the backs of the angles were fixed in the model.

To model the applied load, pressure loads were applied every 6.0 in. across the elements of the top flange. Pressure loading was chosen so that the applied force would remain normal to the flange regardless of flange rotation, which more accurately modeled experimental conditions. Because the pressure loading was all in the vertical direction, two 0.01-kip perturbation forces out of the plane and normal to the web were applied in the e' region and first web-post to assist buckling. The purpose of these small perturbation forces was to ensure that when the models became unstable, buckling would ensue. The locations for the perturbation forces were determined by an eigenvalue buckling analysis completed in ANSYS (Hennessey et al., 2004), which predicts the theoretical buckling strength and corresponding buckled shapes for multiple buckling modes of the beam.

Once all the boundary conditions were specified, the model was solved using a large displacement static analysis. Load was applied incrementally until the model became unstable. For model correlation, the analysis also considered linear elastic service load conditions.

Model Correlation

Strain gage data taken in the e' region were compared to the FE strain results to ensure correlation between the model and experimental results. The FE strain results correlated well with the experimental strains. Additionally, the load-deflection behavior of the model was compared to the experimental data. Typical load-deflection plots, comparing analytical models with corresponding experimental specimens, can be seen for castellated and cellular beams in Figures 4a and 4b, respectively. Design loads for all beams were determined using the allowable stress design (ASD) methodology prescribed by SMI. (SMI, 2004) The average value difference between the experimental and analytical deflections at the calculated design load was within 0.05 in. for both castellated and cellular specimens, indicating a close correlation between analytical and experimental results. Correlation between analytical and experimental deflections was also close at the failure load, with only three of the 18 specimens experiencing more than a 0.1-in. difference.

Comparisons of the load-deflection plots for the analytical and experimental specimens showed similar results for all modeled sets with very good correlation between the experimental and analytical near service loads. As the specimens approached failure loads, the FE deflections were, in general smaller than the experimental results, but were still within the range of experimental variability.

Lastly, analytically predicted failure loads were compared to experimental values. This comparison is given in Table 2. The analytical models accurately predict experimental failure loads, with only one specimen exhibiting more than a 10% difference between analytical and experimental failure loads. In most cases, the failure loads were predicted within 5%.

Parametric Study

Once the model was correlated, additional uncoped beams for each depth were analyzed. Note that these additional beams were not tested, only modeled, and that they varied from the tested beam models only by cope dimension. The uncoped models were identified for each set by the designation (a) [for example, CB 1(a)]. For the 21-in.-deep

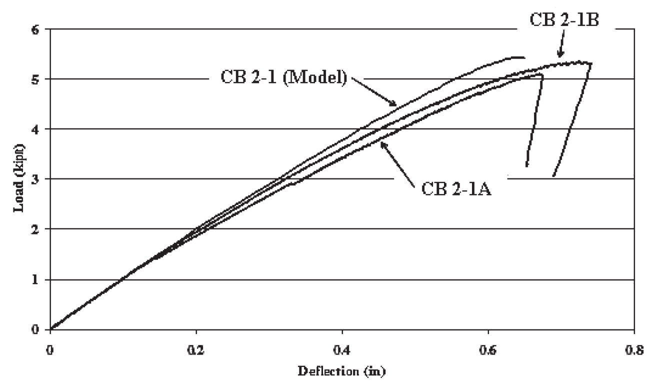

(a) CB 2-1 castellated beam

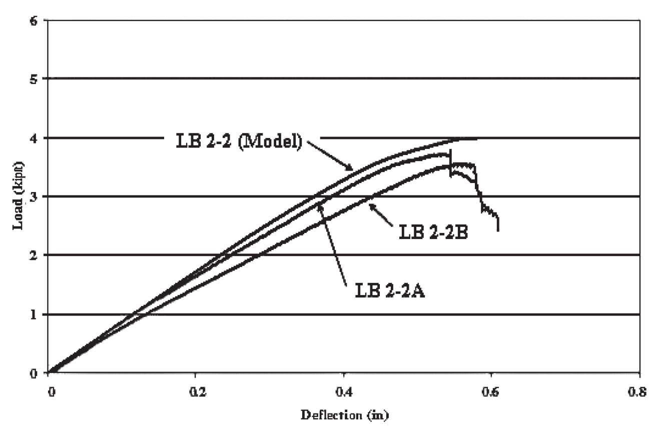

(b) LB 2-2 cellular beam

Fig. 4. Experimental and analytical load vs. deflection results.

Table 2: Experimental and Analytical Beam Failure Loads						
	e´ distance (in)	Top Cope Dimension (length × depth)	Design Load (kip/ft)	Failure Load (kip/ft)		Avg. % Difference for Failure Loads
				Experimental	Model	
Castellated Beams						
CB 1 (a)	9.28	0 × 0	3.0	—	11.0	—
CB 1-1	3.33	3 × 5		9.3 – 9.7	9.6	+1.0
CB 1-3	3.03	3 × 5.5		9.2 – 9.8	9.2	–3.3
CB 1-2	2.47	3 × 6		9.2 – 9.7	9.1	–3.8
CB 2 (a)	11.14	0 × 0	1.8	—	5.9	—
CB 2 (b)	6.59	3 × 3.5		—	5.6	—
CB 2 (c)	5.73	3 × 4.5		—	5.5	—
CB 2-1	4.87	3 × 5.5		5.1 – 5.3	5.4	+3.7
CB 2-2	4.44	3 × 6		5.0 – 5.2	5.3	+3.8
CB 2-3	4.04	3 × 6.5		4.3 – 4.4	4.8	+9.4
CB 2 (d)	3.59	3 × 7		—	4.7	—
CB 3 (a)	12.61	0 × 0	2.8	—	8.5	—
CB 3-1	6.63	3 × 5.5		7.7 – 7.8	7.8	+0.6
CB 3-2	6.15	3 × 5.75		7.4 – 7.6	7.7	+2.6
CB 3-3	5.51	3 × 6.5		6.5 – 6.8	6.9	+3.6
Cellular Beams						
LB 1 (a)	8.38	0 × 0	3.0	—	8.1	—
LB 1-1	2.63	3 × 5		7.6 – 7.7	7.5	–2.0
LB 1-3	2.25	3 × 5.5		7.3 – 7.4	7.5	+0.7
LB 1-2	1.88	3 × 6		7.0 – 7.1	7.3	+3.4
LB 2 (a)	9.88	0 × 0	1.9	—	4.4	—
LB 2 (b)	5.31	3 × 3.5		—	4.3	—
LB 2 (c)	4.50	3 × 4.5		—	4.2	—
LB 2-1	3.69	3 × 5.5		3.7 – 3.8	4.0	+6.3
LB 2-2	3.31	3 × 6		3.6 – 3.8	4.0	+7.5
LB 2-3	2.94	3 × 6.5		3.5 – 3.6	3.8	+6.6
LB 2 (d)	2.63	3 × 7		—	3.8	—
LB 3 (a)	11.19	0 × 0	2.7	—	7.0	—
LB 3-1	5.06	3 × 5.5		5.4 – 5.4	6.6	+18.2
LB 3-2	4.88	3 × 5.75		6.5 – 6.7	6.6	0.0
LB 3-3	4.31	3 × 6.5		5.8 – 5.8	6.4	+9.4

sets, both castellated and cellular, three additional parametric points were modeled. These points consisted of two modeled specimens with smaller copes than the experimental specimens and one modeled specimen with a larger cope than the experimental specimens. The smaller copes that were modeled were 1 and 2 in. smaller than the LB/CB 2-1 specimen copes, respectively. The larger modeled cope was ½ in. larger than the LB/CB 2-3 specimen copes. The additional parametric points for these sets were designated LB/CB 2 (b) – (d). The analytical failure loads for all modeled specimens and their associated cope geometry are presented for the castellated and cellular beams in Table 2.

Member Capacity Reduction vs. e' Distance Reduction

Using the e' distance and failure load from the uncoped models, it was possible to compare the percent reduction in capacity against the percent reduction in e' distance for each model set. For this comparison, the failure load and the e' distance from the uncoped specimens were taken as maximum capacity and maximum e' distance for a given model set. The e' distances and failure loads for all other specimens within the set were then compared to these values to determine the reduction of load capacity as a function of e' distance. The CB 2 and LB 2 sets are presented, though similar results were found for all six model sets (Hennessey et al., 2004). The percent of maximum capacity versus percent of maximum e' distance for these modeled specimens is shown in Figure 5.

Similar to the experimental results, Figure 5 indicates a clear reduction in capacity as the e' distance is reduced. However, when shown as a percentage of the maximum e' distance, it can be seen that extremely large copes are required before capacity loss becomes significant. For both castellated and cellular model specimens, reductions in the e' distance of 50% result in less than a 10% loss in capacity. As the e' distance reaches one-third of the maximum e' distance (in other words, approximately two-thirds of the e' material of the uncoped beam is removed), the capacity loss becomes as much as 20% for castellated beams. Yet even with this capacity reduction, all beams failed at a load at least 1.8 times its design load (ASD method). Cellular beams sustained less capacity loss on a percentage basis than did castellated beams for similar percent reductions in e' distance.

Failure Modes

All specimens in the experimental program failed in some combination of e' region buckling and buckling of the first web-post. However, because these two buckling modes occurred almost simultaneously, it was difficult to determine visually the dominant failure mode. This combination buckling can be seen for a castellated beam in Figure 6a and for a cellular beam in Figure 6b.

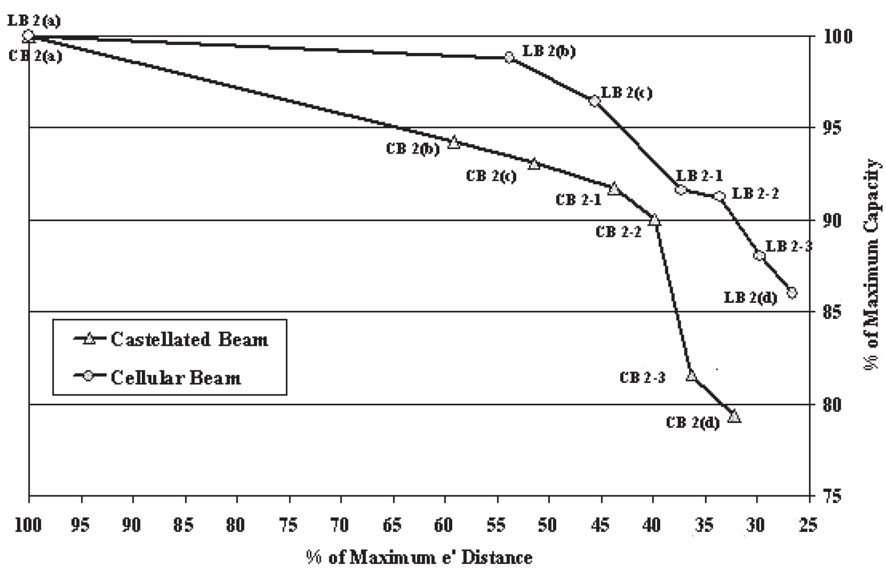

Fig. 5. Percentage of capacity reduction vs. percentage of e´ distance reduction (analytical).

The failure modes for the analytically modeled specimens all incorporate the same critical regions as the experimental results: e' region and first web-post. However, with the analytical specimens it is possible to determine the interaction between the two buckling modes and to differentiate which region precipitated the beam's failure. Sample failure modes for the CB 2 and LB 2 specimens are shown in Figures 7 and 8, respectively, where the out-of-plane buckling locations observed during analytical modeling are illustrated for the specimens. The graphs to the left of each of the FE displacement plots give the load and magnitude of the out-of-plane deflection and the degree of interaction between the buckling modes in the e' region and the first web-post. For each model shown, out-of-plane deflections are graphed at four locations: e' region (Point A), bottom of the first web-post (Point B), middle of the first web-post (Point C), and top of the first web-post (Point D). The locations of the points shown in the graphs are identified on the associated beam model. Note that the dark contours on the FE out-of-plane displacement plots refer to the extreme out-of-plane displacements (both maximum and minimum) for that particular plot.

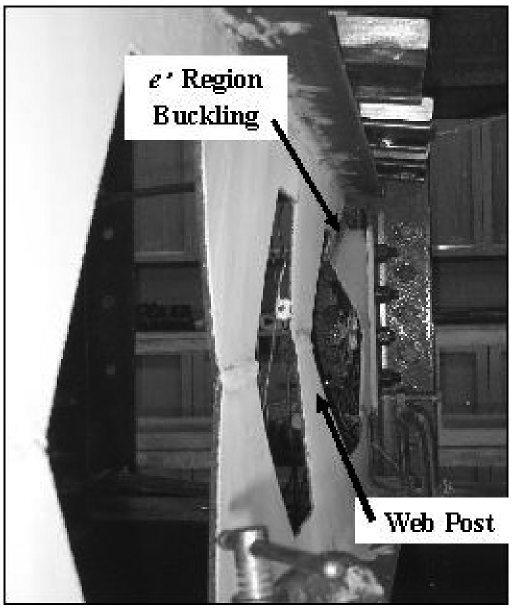

(a) Castellated beam

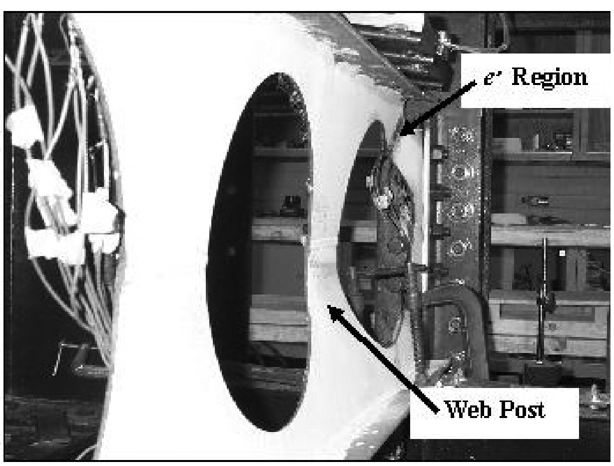

(b) Cellular beam

Fig. 6. Experimental buckling modes.

Despite the varying degree of contribution from the first web-post, the e' region generally becomes the dominant failure mode as the e' dimension is reduced, as indicated in Figure 7. The uncoped model (Figure 7a) experienced buckling in the first web-post with no influence from the e' region. Note that the opposite directions for the out-of-plane (Uz) deflections at Points B and D indicate an S-shaped buckling of the web-post. As the e' region was reduced, the influence of the e' region on the beam's failure became more significant. The modeled specimen with the largest cope for this set (e' distance of 3.59 in.) experienced a failure mode that was primarily e' buckling with some S-shaped first web-post buckling (Figure 7c). As seen in Figure 7b, modeled specimen CB 2-2 represents a transition in buckling mode interaction. The graph of out-of-plane deflections indicates that although the web-post deflected more at failure, the e' deflections were greater for the majority of the test. All specimens modeled with larger copes than CB 2-2 indicated e' buckling being dominant throughout the tests. Comparison of this data with Figure 5 shows that the greater the influence of the e' region on the specimens failure, the lower the member capacity.

As shown in Figure 8, the LB 2 model set showed very similar failure mode results to the CB 2 model set. The uncoped model specimen (Figure 8a) experienced an S-shaped buckling in the first web-post with no contribution from the e' region. As the cope size was increased, the model specimens began to fail in a combination of the two primary buckling modes (Figure 8b), with the contribution from the e' becoming more significant with increasing cope size. The LB 2 model with the largest cope (e' distance of 2.61 in.) failed almost entirely due to buckling in the e' region (Figure 8c). This localization of out-of-plane displacement at e' caused by the very small e' distance is responsible for the markedly different appearance in the FE displacement plot of Figure 8c. In the case of e' only buckling, large out-of-plane deflection occurs in e' only. Due to the absence of an S-shaped buckling mode in the first web-post, the other displacement extreme is zero out-of-plane displacement, which can be seen in the dark shading of the rest of the beam.

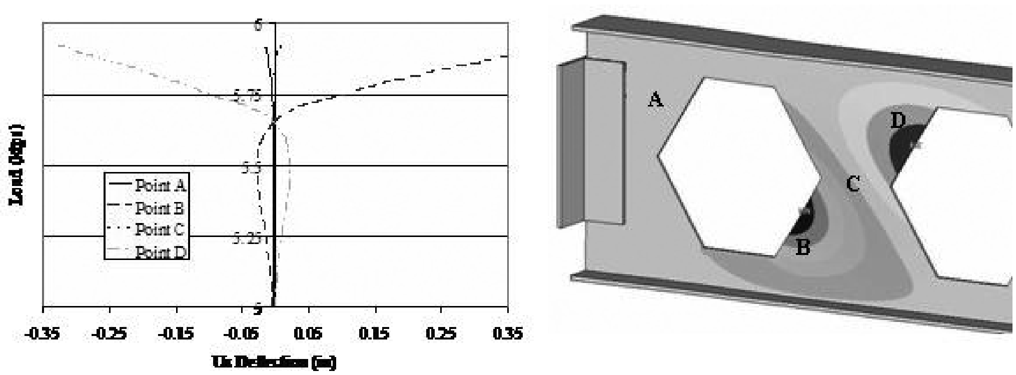

(a) CB 2 (a): no cope

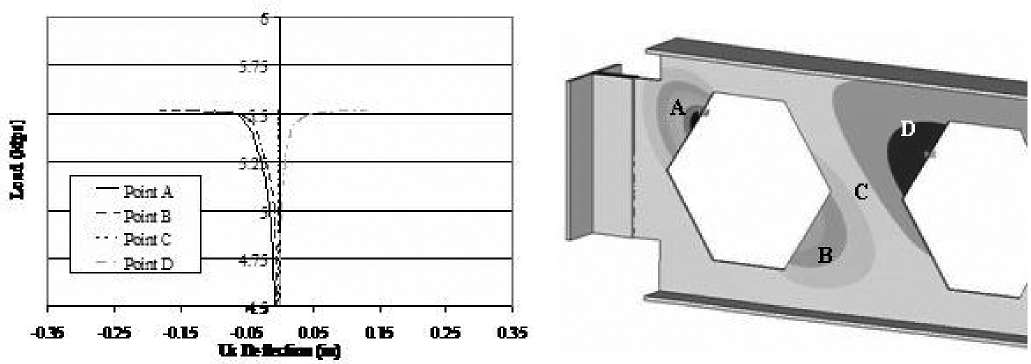

(b) CB 2-2: 6-in. cope

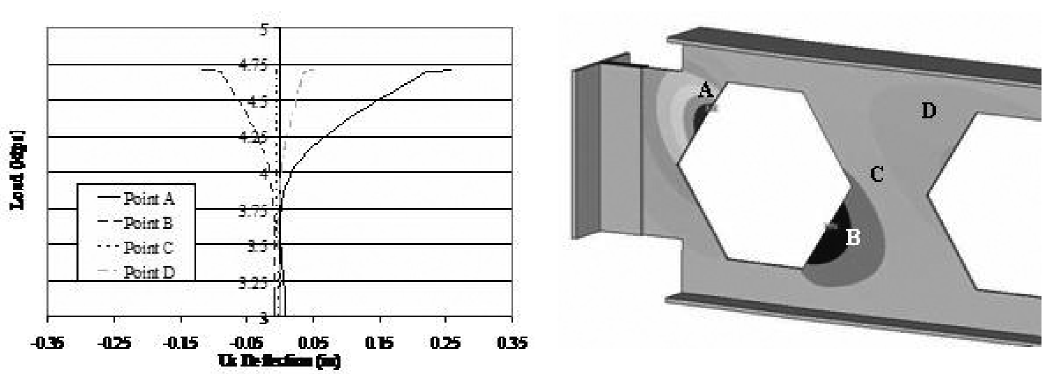

(c) CB 2 (d): 7-in. cope

Fig. 7. 21-in. castellated beam (CB 2) buckling modes for various cope depths. Note: Uz refers to out-of-plane deflection.

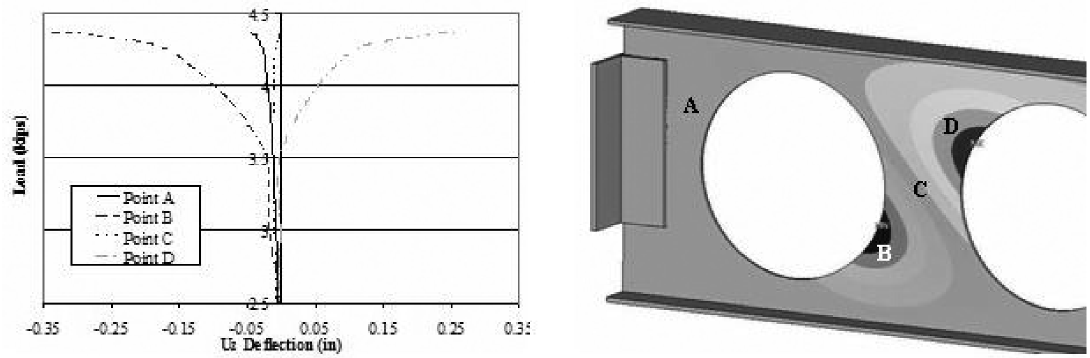

(a) LB 2 (a): no cope

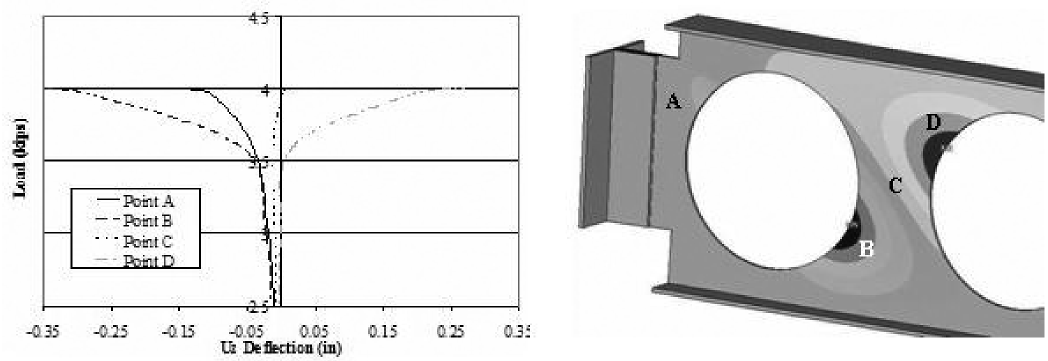

(b) LB 2-1: 5.5-in. cope

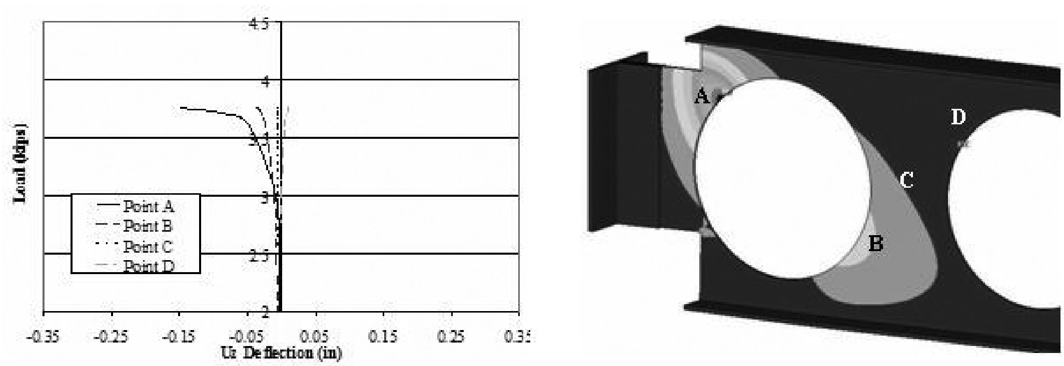

(c) LB 2 (d): 7-in. cope

Fig. 8. 21-in. cellular beam (LB 2) buckling modes for various cope depths. Note: Uz refers to out-of-plane deflection.

CONCLUSIONS

Gaining a better understanding of how buckling behavior is affected by e' distance will aid in design and analysis of castellated and cellular beams. The objective of this study was to examine the effect of cope geometry and e' distance on the strength and behavior of noncomposite, uniformly loaded 15 ft. castellated and cellular steel beams of 18-, 21- and 24-in. depths. The beams in this study all had double-angle connections. Other connection types typically used in practice need to be investigated.

Utilizing the analytical and experimental results from the research program, the following conclusions were drawn about the effect of cope geometry on various aspects of the behavior of castellated and cellular beams:

1. Although reduction in the e' distance clearly reduces the member capacity, large percentage reductions in the e' distance are required before capacity loss becomes significant. All modeled sets indicated that a 50% reduction of the e' distance resulted in less than a 10% reduction in capacity.

2. All specimens, even specimens with the largest copes, experienced failure loads significantly above (>1.8) design values (ASD). (See Table 2.)

3. The detrimental effect of reduced e' distance on the overall beam capacity was less for the cellular beams (13.6% maximum capacity reduction) than for the castellated beams (20.3% maximum capacity reduction).

4. As the size of the cope was increased, the contribution of the e' region in the failure of the beam became more significant.

5. The greater the influence of the e' region on the beam's failure, the more dramatic the decline in capacity.

ACKNOWLEDGMENTS

The authors gratefully acknowledge the financial support of SMI Steel Products, and the technical support of Joe Pote and Sameer Fares from SMI. The assistance of George Pappas, Civil Engineering Lab Technician, was invaluable, as were the efforts of undergraduate research fellows, Geoffrey Morrissey and Michael Illgas.

REFERENCES

Aglan, A.A. and Redwood, R.G. (1974), "Web Buckling in Castellated Beams," *Proceedings of the Institution of Civil Engineers (London). Part 1—Design & Construction*, Vol. 57, June, pp. 307–320.

Aloi, N., Gross, S., Dinehart, D., and Yost, J. (2002), "Experimental Tests of Singly- and Doubly-Symmetric Noncomposite Castellated Beams," Research Report 1 to SMI Steel Products, Villanova University.

ASTM (1989), "Standard Test Method of Tension Testing of Metallic Materials," ASTM E8-89B, American Society of Testing Materials.

Blodgett, O. (1966), *Design of Welded Structures*, Cleveland, Ohio: Lincoln Arc Welding Foundation.

Boyer, J.P. (1964), "Castellated Beams-New Developments," *Engineering Journal*, Vol. 1, No. 3, pp. 104–108.

Douty, R.T. and Baldwin, J.W. (1966), "Measured and Computed Stresses in Three Castellated Beams," *Engineering Journal,* Vol. 3, No. 1, pp. 15–18.

Gibson, J. and Jenkins, W. (1957), "Investigation of the Stresses and Deflections in Castellated Beams," *The Structural Engineer*, December, pp. 467–479.

Hennessey, J., Dinehart, D., Hoffman, R., Gross, S., and Yost, J. (2004), "Effect of Cope Geometry on the Strength and Failure Behavior of Non-Composite Open Web Expanded Beams," Research Report 6 to SMI Steel Products, Villanova University.

Hosain, M.U. and Speirs, W.G. (1973) "Experiments on Castellated Steel Beams," *Supplement to the Welding Journal*, August, pp. 329–342.

Kolosowski, J. (1964) "Stresses and Deflections in Castellated Beams," *The Structural Engineer*, January, pp. 19–24.

Mandel, J., Brennan, P., Wasil, B., and Antoni, C. (1971), "Stress Distribution in Castellated Beams," *Journal of the Structural Division*, July, pp. 1947–1967.

Redwood, R. and Demirdjian, S. (1998), "Castellated Beam Web Buckling in Shear," *Journal of Structural Engineering*, October, pp. 1202–1207.

Reiter, M., Dinehart, D., Gross, S., and Yost, J. (2002), "Experimental Tests of Non-Composite Cellular Beams," *Research Report 2 to SMI Steel Products*, Villanova University.

SMI Steel Products (2004), *Design Guide for Castellated and Cellular Beams*.

Surtees, J.O. and Liu, Z. (1995), *Report of Loading Tests on Cellform Beams: Research Report,* University of Leeds.

Toprac, A.A. and Cooke, B.R. (1959), "An Experimental Investigation of Open-Web Beams," *Welding Research Council Bulletin Series No.47*.

Ward, J.K. (1990), *Design of Composite and Non-Composite Cellular Beams*, Steel Construction Institute, Berkshire.

Zaarour, W. and Redwood, R. (1996), "Web Buckling in Thin Webbed Castellated Beams," *Journal of Structural Engineering,* August, pp. 860–866.